

# *Influence of granulate and pressure on green compacts and the current-voltage characteristics of sintered ZnO-based varistor ceramics*

*Slavko Bernik<sup>1</sup>, Matejka Podlogar<sup>1</sup>, Saša Rustja<sup>2</sup>, Mirjam Cergolj<sup>2</sup>*

<sup>1</sup>*Jožef Stefan Institute, Ljubljana, Slovenia*

<sup>2</sup>*VARSIS d.o.o., Ljubljana, Slovenia*

**Abstract:** Granulates G1, G2 and G3, having the same varistor composition but different morphologies in terms of shape, size and size distribution, were characterized for their compactness and flow characteristics. They were also examined during the preparation of disc-shaped green pieces with a diameter of 20 mm by uniaxial pressing at pressures from 3.2MPa to 300MPa. The density and strength of the green samples showed similar pressure dependencies for all the granulates and for the same pressure the green densities were similar. The density of the varistor ceramics sintered at 1200 °C for 2 hours showed little dependence on the compression pressure and the used granulate due to sintering in the presence of a Bi<sub>2</sub>O<sub>3</sub>-rich liquid phase; they already had 93% of theoretical density when pressed at only 10MPa, while for higher pressures the density increased to 96%. The pressure applied during uniaxial pressing also had a small influence on the current-voltage (I-U) characteristics of the varistor ceramics. The varistor ceramics from granulate G1 with the preferred morphology of the granules showed a higher threshold voltage (U<sub>T</sub>) and better I-U nonlinearity (higher coefficient of nonlinearity a) than the ceramics produced from granulates G2 and G3.

**Keywords:** ZnO; varistor ceramics; granulate morphology; compression pressure; strength; electrical properties

## *Vpliv granulata in pritiska na zelene oblikovance in tokovno-napetostne karakteristike sintrane varistorske keramike na osnovi ZnO*

**Izvleček:** Analizirali smo kompaktnost in tečljivost granulotov G1, G2 in G3, ki imajo enako varistorsko sestavo in različno morfologijo granul glede oblike, velikosti in porazdelitve velikosti. Preverili smo vpliv granulata na pripravo zelenih kosov v obliki diska s premerom 20 mm pri enosnem stiskanju s pritiski od le 3,2MPa do 300MPa. Pri vseh granulatih se je pokazala podobna odvisnost gostote in trdnosti zelenih oblikovancev od pritiska stiskanja in pri enakem pritisku so imeli podobno gostoto. Gostote varistorske keramike, sintrane pri 1200 °C 2 uri, so pokazale majhno odvisnost od pritiska stiskanja in granulata, kar je posledica sintranja v prisotnosti tekoče faze Bi<sub>2</sub>O<sub>3</sub>; keramika je imela 93% teoretično gostoto že pri stiskanju oblikovancev s pritiskom 10MPa, pri višjih pritiskih stiskanja pa je gostota narasla na 96%. Pritisk enosnega stiskanja ima dokaj majhen vpliv tudi na tokovno-napetostne (I-U) lastnosti varistorske keramike. Varistorska keramika iz granulata G1 z zeleno morfologijo granul je imela višjo prebojno napetost (U<sub>T</sub>) in boljše nelinearnost I-U (višji koeficient nelinearnosti a) kot keramika iz granulotov G2 in G3.

**Ključne besede:** ZnO; varistorska keramika; morfologija granulata; pritisk stiskanja; trdnost; električne lastnosti

\* Corresponding Author's e-mail: [slavko.bernik@ijs.si](mailto:slavko.bernik@ijs.si)

### *1 Introduction*

An exceptional current-voltage (I-U) nonlinearity and a high energy-absorption capability are the reasons why ZnO-based varistors are widely used in the protection of electrical devices, electronic circuits and power sys-

tems against impulse voltage transients over a broad range from a few volts up to several 100 kV. The unique characteristics of ZnO-based varistor ceramics are closely related to their microstructure and arise from the combined effects of the I-U nonlinearity of the

grain boundaries and the high conductivity of the ZnO grains. The nonlinearity results from the electrostatic barriers, which ideally have a breakdown voltage of about 3.2V and are induced by the presence of a  $\text{Bi}_2\text{O}_3$  layer at the grain boundaries. The high conductivity of the grains is obtained by doping the ZnO with oxides of Co, Mn and Ni. The size of the ZnO grains determines the number of grain boundaries at a certain thickness of the ceramic and hence its breakdown voltage, which is the sum of the breakdown voltages of all the non-linear grain boundaries.[1,2] Control of the grain size is therefore important when tailoring the breakdown voltage of the varistor ceramics; hence, either  $\text{Sb}_2\text{O}_3$  or  $\text{TiO}_2$  are usually added to prepare fine-grained, high-voltage or coarse-grained, low-voltage ceramics, respectively.[3] Accordingly, the starting composition of the varistor powder mixture is rather complex, as typically up to about 10% by weight of Bi, Sb, Co, Mn, Ni and Cr oxide is added to the ZnO powder. In the process of sintering at a temperature of about 1200 °C, a complex microstructure is developed, typically composed of the ZnO phase and the secondary phases, the  $\text{Bi}_2\text{O}_3$ -rich phase, the  $\text{Zn}_7\text{Sb}_2\text{O}_{12}$ -type spinel phase and the  $\text{Bi}_3\text{Zn}_2\text{Sb}_3\text{O}_{14}$ -type pyrochlore phase, which has to support the I-U characteristics as required by a particular application. However, sintering is only the final step in processing the varistor ceramics and in such a complex system regarding its chemical composition and the electrical properties, the entire previous history of preparation, especially the proper homogenization of the starting powder mixture for chemical (i.e., compositional) homogeneity and compaction (i.e., pressing) of green molds, also has a strong influence on the final physical properties, much more than with the simpler systems. [4,5]

In the processing of varistors, pieces of varistor ceramic with various dimensions are usually prepared using a standard powder metallurgy procedure with uniaxial pressing of the granulate. Under laboratory conditions, smaller pieces of ceramic can be shaped by pressing the powder or a mixture of powders without or, if necessary, with adding a binder to improve the compressibility and to prevent the formation of cracks or, in the extreme, layering due to internal stresses. The process of shaping must ensure the required repeatability in the production of green bodies without defects, which is requirement in order to obtain ceramics without defects also after sintering. Even with slightly larger samples and in large-scale production this cannot be ensured without the use of granulate, the characteristics of which become the determining factor. The use of a granulate with the appropriate mechanical properties is therefore necessary for the optimization of the pressing process. Spray-drying of the suspension (i.e., the slurry) is typically used in the processing of granu-

late; its characteristics (shape, size, size distribution, density, packing, mechanical strength) are strongly affected by the characteristics of the suspension, which also has to ensure the compositional homogeneity. The granulate must provide excellent compressibility, which means achieving the maximum green density using the lowest possible pressure and an adequate uniformity required for the production of green molds without defects. In order to provide unique compression properties, it is desirable that the granules are round and have a smooth surface. In order to understand what kind of granulate and what kind of granulate properties are required, the processes and mechanisms of granulate deformation during compression need to be known.[6-17]

The pressing of granules usually involves plastic and/or viscoelastic deformations. In the plastic material, the boundary of elasticity, when the material returns to its original condition after load removal, is rapidly reached; with a further load there are irreversible changes. The viscoelasticity is reflected in the viscous and elastic properties. The viscous material resists the load and the strain in material is linearly increasing with the load time. The elastic material, however, deforms under load, but when the load is removed, it can return to its original condition. In the case of granules that exhibit plastic deformation and have different mechanical strengths, some are crushed under the pressure, while those with greater mechanical strength remain whole and cause the formation of a heterogeneous structure with defects. On the other hand, perfectly viscous granules would form perfectly close packing without an applied pressure. This implies that the viscoelastic behavior plays an important role in the compaction process of the granulate. In the process of pressing granulate, first, at low levels of compression pressure, rearrangement of the granules occurs, so that the gaps between them are filled. A further increase in the pressure level tends to increase the remaining tension due to fracture or deformation of the granules. From the viscoelastic deformation of granules, the process of stress release results, which depends on the characteristics of the granules. Thus, the binder-free granules have a lower viscoelastic deformation than those having a binder, which indicates that the compressibility is highly dependent on the binder. With a further increase in the compression pressure, the relaxation tension of the granules increases, thereby increasing the packing density.[6-17]

The influence of the morphology of the granules on the compression quality is reflected in the bending strength of the pieces of ceramic. A higher bending strength comes from ceramics with higher density. A granulate of full granules with a spherical morphology, which allows the preparation of pieces with a higher green density, can contribute to the higher bending strength of ceramics. However, the results showed that a higher density of granules

tends to reduce their compressibility. In the case of green bodies with a density virtually identical to the density of the granules, apparently there was no deformation of the granules in the process of compression; such pieces are non-homogeneous and contain defects that greatly impair the strength of sintered ceramics. The lower-density granules must break down in the compression process to form a homogeneous and compact body. The most appropriate is therefore granulate from spherical and full granules, which exhibit the highest relaxation stress as a result of the viscoelastic deformation; it is a granulate having a lower density of full granules, so that the difference in density between the granules and the green body is a maximum.[6-17]

In this work granulates with different morphologies and same varistor composition were characterized for bulk and tapped density. Their flow characteristics were also determined from the compressibility index and the Hausner ratio. Furthermore, their characteristics when uniaxially pressed were analyzed for pressures ranging from 3.2 MPa to 300 MPa by determining the density and strength of their green compacts. Finally, the influence of the granulate and the compaction pressure on the density and I-U characteristics of ceramics sintered at 1200 °C for 2 hours was studied.

## 2 Experimental

In the study the varistor granulates G1, G2 and G3 with different morphological characteristics were examined and used for the preparation of ZnO-based varistor ceramics. The granulates were prepared using the same spray-drying conditions from stable water slurries having the same composition and amount of varistor powder mixture (i.e., ZnO powder doped with oxides of Bi, Sb, Co, Mn, Ni and Cr) but a different amount of added binder. The bulk density ( $r_0$ ) of the granulates was obtained by adding a known mass ( $m$ ) of granulate to a graduated cylinder to determine the unsettled apparent volume (bulk volume,  $V_0$ ). By mechanically tapping a graduated cylinder containing the sample until little further volume change is observed to obtain the final tapped volume ( $V_F$ ) the tapped density ( $r_F$ ) was obtained. The flow characteristics of the granulates were estimated from the compressibility index (i.e., the Carr index) and the Hausner ratio. The compressibility index was determined using the expression  $Ci = 100(V_0 - V_F)/V_0$  (in %) and the Hausner ratio as  $H_r = V_0/V_F$ . From the studied granulates disc-shaped green compacts having a mass of 3g and a diameter of 20 mm were uniaxially pressed in a stainless-steel die at different pressures of 3.2 MPa, 10 MPa, 50 MPa, 100 MPa, 150 MPa, 200 MPa and 300 MPa. Their green density and strength were determined with respect to the compacting pressure to assess

the influence of the granulate's characteristics. The biaxial flexural strengths of the green samples were measured with a piston-on-three-balls set up, according to the ISO 6872 standard, on a universal testing machine (Quasar 50; Galdabini, Varese, Italy) at a loading rate of 1 mm/min. Microstructures of the fractured surfaces of green pieces shaped at different pressures from granulate G1 after a strength analysis were examined on a scanning electron microscope (SEM, JSM-5800, JEOL, Japan). Green compacts from all the studied granulates and pressed with different pressures were sintered in air at a temperature of 1200 °C for 2 hours. Their sintered densities (as well as their green densities) were measured using a density-measurements system Densitac (Metar sa, Matran, Switzerland). For the DC current-voltage (I-U) characterization, silver electrodes were painted on both parallel surfaces of the discs and fired at 600 °C. The nominal varistor voltages ( $U_N$ ) at 1mA/cm<sup>2</sup> and 10mA/cm<sup>2</sup> were measured using a Keithley 2410 Digital SourceMeter, and the threshold voltage  $U_T$  (V/mm) and the non-linear coefficient  $\alpha$  were determined. The leakage current ( $I_L$ ) was measured at 0.75 $U_N$  (1mA/cm<sup>2</sup>).

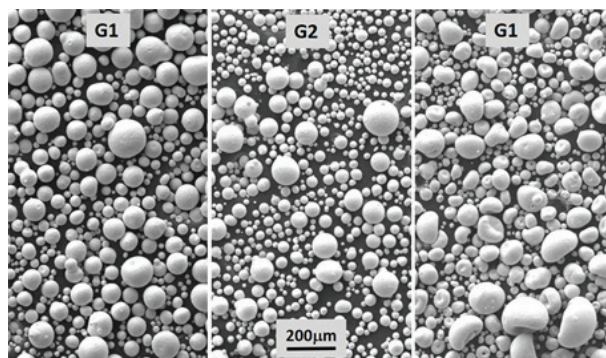


**Figure 1:** SEM images of varistor granulates G1, G2 and G3 showing differences in their morphology.

## 3 Results and discussion

The varistor granulates examined in this work and used for the preparation of the ZnO-based varistor ceramics are shown in Fig. 1. The differences in their morphologies are clearly evident. The granulate G1 has nice spherical granules with quite a uniform size distribution in the range from the smallest of about 10 µm to the largest of about 200 µm. In the granulate G2 the sizes of the smallest and the largest granules are similar to G1; however, the share of smaller granules with sizes in the range from 10 µm to about 50 µm is evidently dominating. The granulate G3 has granules with similar sizes and size distribution as G1; however, the granules have imperfect shapes, often with a crater. While the smaller

granules are full, the larger granules can be either hollow or full in all three granulates, as can be seen in Fig. 2.

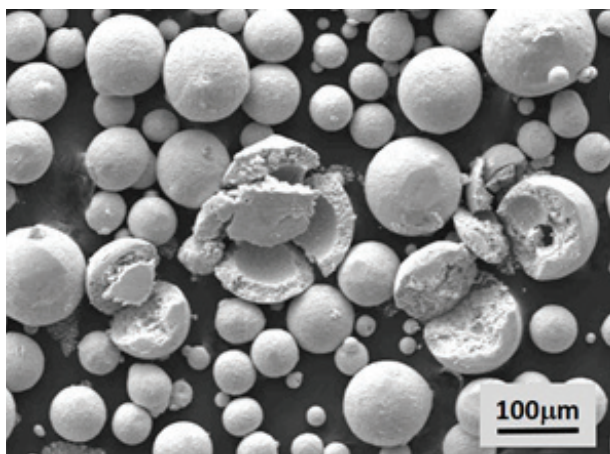


**Figure 2:** SEM image showing that granules, especially larger ones could be either full or hollow.

Table 1 lists the bulk ( $r_o$ ) and tapped ( $r_f$ ) densities of the granulates as well as their flow characteristics estimated from the compressibility index ( $C_i$ ) index and the Hausner ratio ( $H_R$ ) in accordance to the scale given in Table 2. [18] The granulate G1 with a perfect spherical morphology and uniform size distribution of the granules has the highest bulk and tapped densities and an excellent flow characteristic. The granulate G2, which also has perfectly spherical granules, but non-uniform size distribution (i.e., the proportion of small granules predominates), has lower bulk and tapped densities than G1. Nevertheless, according to  $C_i$  and  $H_R$  its flow characteristic is still excellent. However, the granulate G3 with a deformed shape of the granules but a uniform size distribution has similar bulk and higher tapped density than G2, and in regard to its higher  $C_i$  and  $H_R$  values, one level poorer flow properties, classified as good.

**Table 1:** Bulk ( $r_o$ ) and tapped ( $r_f$ ) density of granulates, and their compressibility index ( $C_i$ ) and Hausner ratio ( $H_R$ ) for an estimation of the flow characteristics with respect to the scale given in Table 2

| Granulate | $V_o$ (ml) | $V_f$ (ml) | $\rho_o$ (g/ml) | $\rho_f$ (g/ml) | $C_i$ (%) | $H_R$ | Flow character |
|-----------|------------|------------|-----------------|-----------------|-----------|-------|----------------|
| G1        | 23.25      | 21.25      | 1.10            | 1.20            | 8.6       | 1.09  | excellent      |
| G2        | 25.00      | 23.00      | 1.02            | 1.11            | 8.0       | 1.09  | excellent      |
| G3        | 25.05      | 22.00      | 1.02            | 1.16            | 12.2      | 1.14  | good           |

Regardless of their morphological differences and the differences in their compactness and flow characteristics, all the granulates enable the uniaxial pressing of disc-shaped green compacts with a diameter of 20 mm across a broad range of pressures from the lowest of only

3.2 MPa to the highest of 300 MPa without any difficulties; even after pressing with the lowest pressures the green compacts from all the granulates were compact enough for subsequent handling without any problem and at the highest pressure no lamination of the discs was observed. The density of the green compacts from the granulate G1 with respect to the pressure of the uniaxial pressing is given in Fig. 3; the density rapidly increased with pressure up to 50 MPa to about 3 g/cm<sup>3</sup>, while with further increasing of pressure the density increased steadily to the value of about 3.6 to 3.7 g/cm<sup>3</sup> at 300 MPa. Practically same green densities for the given pressure and the same dependence of the green density on the pressure were obtained also for the granulates G2 and G3.

**Table 2:** Flow properties of solids with respect to their Carr index (i.e., compressibility index) and Hausner ratio.[18]

| Carr's index (%) | Flow character  | Hausner ratio |
|------------------|-----------------|---------------|
| 1-10             | Excellent       | 1.00-1.11     |
| 1-15             | Good            | 1.12-1.18     |
| 16-20            | Fair            | 1.19-1.25     |
| 21-25            | Passable        | 1.26-1.34     |
| 26-31            | Poor            | 1.35-1.45     |
| 32-37            | Very poor       | 1.46-1.59     |
| >38              | Very, very poor | >1.60         |

The strengths of the green pieces prepared at different pressures of uniaxial pressing are given in Fig. 4. All the granulates show a similar dependence of the strength on the pressure. However, while the samples from granulates G2 and G3 have similar strengths at all pressures, it is higher for the samples from granulate G1 and the difference increases with increasing pressure. After pressing with 300 MPa the samples G1 have a strength of about 17 MPa and the samples G2 and G3, of about 13 MPa.

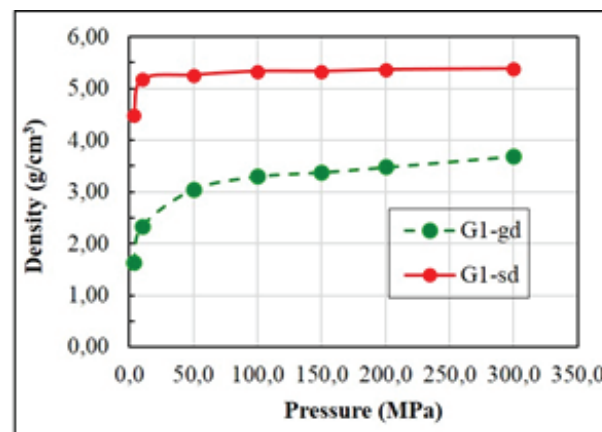


**Figure 3:** Green-density (G1-gd) and density after sintering at 1200 °C (G1-sd) of samples from the granulate G1 with respect to the pressure of uniaxial pressing.

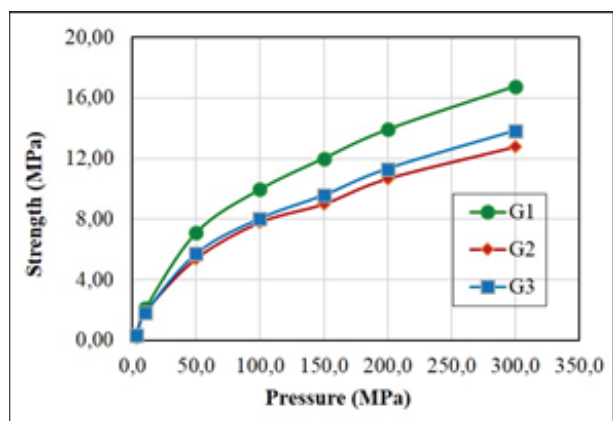


**Figure 4:** Strength of the green compacts from granulates G1, G2 and G3 with respect to the pressure of uniaxial pressing.

Microstructures of a fractured surface of the green samples from the granulate G1, uniaxially pressed at different pressures are presented in Fig. 5. After a pressure of 3.2 MPa the granules remain whole, while being slightly indented into each other so that porosity among them is still evident, which still ensures sufficient compactness for the green samples to be handled without difficulties. At a pressure of 10 MPa the shape of the individual granules is still clearly evident, the degree of indentation among the granules is already much larger so that the remaining porosity among them is already much lower and some granules are already partially collapsed. However, already after a pressure of 50 MPa the microstructure of the fractured surface is perfectly homogeneous as all the granules are fully collapsed so that their shape was not distinct anymore. With a further increase of the pressure the microstructure of fractured surface remains the same.

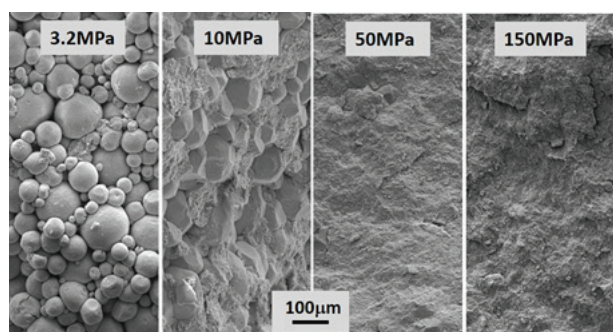


**Figure 5:** Microstructures of fractured surface of green samples pressed from granulate G1 at different pressures.

The densities of the varistor ceramics from the granulate G1, uniaxial pressed at different pressures and sintered at 1200 °C for 2 hours, are graphically presented in Fig. 3. Interestingly, already the samples pressed with only 3.2 MPa had a sintered density of about 4.5 g/cm<sup>3</sup> (i.e.,

about 80% of theoretical density). However, for a pressure of just 10 MPa the density of the sintered ceramics increased to about 5.2 g/cm<sup>3</sup> (93 % t.d.) and with further increasing of the pressure this only slightly increased to about 5.4 g/cm<sup>3</sup> (96 % t.d.). The sintered ceramics from the granulates G2 and G3 had a similar density at a certain pressure and a similar dependence of the density on the compression pressures as the ceramics from the granulate G1. Such results, which showed very little influence of the granulate morphology and the pressure of uniaxial pressing on the density, could be explained by the sintering of the varistor ceramics, which takes place in the presence of the Bi<sub>2</sub>O<sub>3</sub>-rich liquid phase.

The current-voltage (I-U) characteristics of the varistor ceramics from granulates G1, G2 and G3, uniaxially pressed at different pressures and sintered at 1200 °C for 2 hours are presented in Figs. 6 and 7. Surprisingly, very little influence of the compression pressure on the I-U characteristics was observed. Only in the ceramics pressed with 3.2 MPa were noticeably different values of the threshold voltage ( $U_T$ ) and the coefficient of nonlinearity ( $\alpha$ ) observed, while already for a pressure of 50 MPa and higher they were similar for the ceramics from all three granulates. However, the ceramics from granulate G1 had a higher  $U_T$  (about 125 V/mm) than the ceramics from the granulates G2 and G3 with values around 108 V/mm (Fig. 6). Also, the ceramics from granulate G1 had a much higher  $\alpha$  of about 34 in comparison to values of about 20 for the ceramics from the granulates G2 and G3 (Fig. 7). Actually, in the ceramics from granulate G3 the value of  $\alpha$  increases with a higher compression pressure from 19 at 10 MPa to 23 at 300 MPa. Interestingly,  $\alpha$  in the ceramics from granulates G2 and G3 pressed with only 3.2 MPa is higher (25) than at higher pressures. In varistor ceramics from all the studied granulates the leakage current ( $I_L$ ) is similar in the range from 4 to 8  $\mu$ A, regardless of the pressure of the uniaxial pressing.

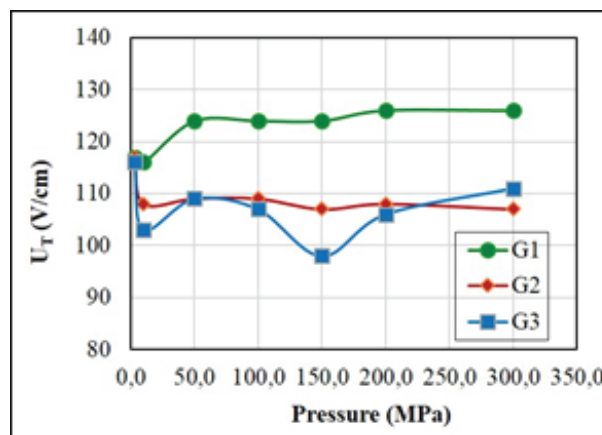


**Figure 6:** Threshold voltage  $U_T$  (V/mm) of the varistor ceramics from granulates G1, G2 and G3, uniaxially pressed at different pressures and sintered at 1200 °C for 2 hours.

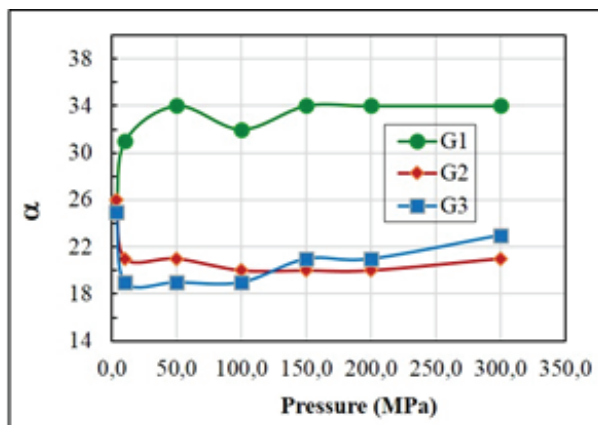


**Figure 7:** Coefficient of nonlinearity  $\alpha$  of the varistor ceramics from granulates G1, G2 and G3, uniaxially pressed at different pressures and sintered at 1200 °C for 2 hours.

## 4 Conclusions

In this work granulates G1, G2 and G3, having the same composition of the varistor powder mixture and different morphologies of the granules, were characterized for their compacting and flow characteristics. Granulate G1 with a uniform size distribution of spherical granules had the highest bulk and tapped densities, and according to the Carr index ( $C_i$ ) and Hausner ratio ( $H_R$ ) they also had excellent flow characteristics. The granulate G2 with the spherical granules but the non-uniform size distribution due to a dominant fraction of smaller granules also had excellent flow characteristics, while the granulate G3 with a uniform size distribution but deformed granules qualified for flow characteristic as good. All the granulates showed good properties in terms of the uniaxial pressing of green bodies for pressures in the range from only 3.2 MPa to 300 MPa; green pieces could be handled without difficulties and no lamination occurred. For all the granulates the density and strength of green samples showed similar dependence to the pressure and for the same pressure the green densities were similar. The samples from G1 with a preferred morphology of the granules had a higher strength. The density of varistor ceramics sintered at 1200 °C for 2 hours showed very little dependence on the compression pressure and the granulate used, and reached 93% of the theoretical density already when pressed with only 10MPa, while for higher pressures the density increased to 96%. This could be explained by the sintering of the varistor ceramics in the presence of the  $\text{Bi}_2\text{O}_3$ -rich liquid phase. Accordingly, also a relatively low influence of compression pressure on the current-voltage (I-U) characteristics of the varistor ceramics was observed. However, the varistor ceram-

ics from the granulate G1 showed a higher threshold voltage ( $U_T$ ) and a better I-U nonlinearity (higher coefficient of nonlinearity  $\alpha$ ) than the ceramics from the granulates G2 and G3. The reasons can be found in their microstructure, which should be thoroughly examined in the future.

## 5 References

1. T. K. Gupta, Application of zinc oxide varistors, *J. Am. Ceram. Soc.*, vol. 73, no. 7, pp. 1817-1840, 1990.
2. D. R. Clarke, Varistor ceramics, *J. Am. Ceram. Soc.*, vol. 82, no. 3, pp. 485-502, 1999.
3. S. Bernik, N. Daneu, A. Rečnik, Inversion boundary induced grain growth in  $\text{TiO}_2$  or  $\text{Sb}_2\text{O}_3$  doped ZnO-based varistor ceramics, *J. Eur. Ceram. Soc.*, vol. 24, pp. 3703-3708, 2004.
4. M. Inada, Formation Mechanism of nonohmic zinc oxide ceramics, *Jpn. J. Appl. Phys.*, vol. 19, no. 3, pp. 409-419, 1980.
5. M. L. Arefin, F. Raether, D. Dolejš, A. Klimera, Phase formation during liquid phase sintering of ZnO ceramics, *Ceram. Int.*, vol. 35, pp. 3313-3320, 2009.
6. J. Tsubaki, H. Yamakawa, T. Mori, H. Mori, Optimisation of granulates and slurries for press forming, *J. Ceram. Soc. Jpn.*, vol. 110, no. 10, pp. 894-898, 2002.
7. M. Naito, Y. Fukuda, N. Yoshikawa, H. Kamiya, J. Tsubaki, Optimisation of suspension characteristics for shaping processes, *J. Eur. Ceram. Soc.*, vol. 17, pp. 251-257, 1997.
8. S. J. Lukasiewicz, Spray-drying ceramics powders, *J. Am. Ceram. Soc.*, vol. 72, no. 4, 617-624, 1989.
9. W. J. Walker Jr., J. S. Reed, S. K. Verma, Influence of slurry parameters on the characteristics of spray-dried granules, *J. Am. Ceram. Soc.*, 82, no. 7, p.p. 1711-1719, 1999.
10. H. Takahashi, N. Shinohara, M. Okumiya, K. Uematsu, T. Junichiro, Y. Iwamoto, H. Kamiya, Influence of slurry flocculation on the character and compaction of spray-dried silicon nitride granules, *J. Am. Ceram. Soc.*, vol. 78, no. 4, p.p. 903-908, 1995 .
11. V. Naglieri, D. Gutknecht, V. Garnier, P. Palmero, J. Chevalier, L. Montanaro, Optimised slurries for spray drying: Different approaches to obtain homogeneous and deformable alumina-zirconia granules, *Materials*, vol. 6, p.p. 5382-5397, 2013.
12. G. Bertrand, P. Roy, C. Filiatre, C. Codder, Spray-dried ceramic powders: A quantitative correlation between slurry characteristics and shapes of the granules, *Ceram. Eng. Sci.*, vol. 60, p.p. 95-102, 2005.

13. K. Uematsu, J. Y. Kim, M. Miyashita, N. Uchida, K. Saito, Direct observation of internal structure in spray-dried alumina granules, *J. Am. Ceram. Soc.*, vol. 73, no. 8, p.p. 2555-2557, 1990.
14. M. Naito, K. Nakahira, T. Hotta, A. Ito, T. Yokoyama, H. Kamiya, Microscopic analysis on the consolidation process of granule beds, *Powder Tech.*, vol. 95, p.p. 214-219, 1998.
15. J. L. Amoros, V. Cantavella, J. C. Jarque, C. Feliu, Fracture properties of spray-dried powder compacts: Effect of granule size, *J. Eur. Ceram. Soc.*, vol. 28, p.p. 2823-2834, 2008.
16. M. I. Zainuddin, S. Tanaka, R. Furushima, K. Uematsu, Correlation between slurry properties and structures and properties of granules, *J. Eur. Ceram. Soc.*, vol. 30, p.p. 3291-3296, 2010.
17. M. Uppalapati, D. J. Green, Effect of relative humidity on the viscoelastic and mechanical properties of spray-dried powder compacts, *J. Am. Ceram. Soc.*, vol. 89, no. 4, p.p. 1212-1217, 2006.
18. R. L. Carr, Evaluating flow properties of solids, *Chem. Eng.*, vol. 72, pp. 163-168, 1965.

Arrived: 31. 08. 2017

Accepted: 15. 11. 2017

